

# Models of Geothermal Areas: New Insights from Electromagnetic Geothermometry



Viacheslav V. Spichak and Olga K. Zakharova

## 1 Introduction

Temperature estimation in the Earth's crust is usually based on temperature logs or heat flow gradient data. Actual measured temperature data are limited to the bore-hole depths amounting in most cases to 1–3 km. Studies of hydrothermal processes showed that specific properties of the underground fluid composition are closely related to the geothermal conditions of their formation.

Therefore, studying these properties provides information about the thermal state of the interior that complements the results of direct thermometry and serves as a basis for forecasting the deep geothermal conditions in scantily explored regions.

The temperature dependency of the composition of some characteristic hydrothermal components is established experimentally with so-called indirect geothermometers. Using empirical or semi-empirical formulas, one can roughly estimate the “base depth” temperature from the known amount or proportion of these components in areas of surface manifestations of thermal activity. Researchers often use indirect estimates based on geological (Harvey and Browne [19]), geochemical [21] or gas composition [2] data to guess the temperature at characteristic depths.

Despite the fact that the aforementioned indirect geothermometers could serve as useful tools for estimating temperatures at some depths and, thus, for constraining the sub-surface temperature, they cannot be used neither for constructing the temperature distribution in the studied area nor for its interpolation / extrapolation from the temperature well logs.

Using the electrical resistivity data of rocks seems to be the most natural approach to indirectly estimate temperature, because this property is commonly a function of

---

V. V. Spichak (✉) · O. K. Zakharova  
Goelectromagnetic Research Centre IPE RAS, Moscow, Troitsk, Russia

temperature. Temperature dependence of the electrical resistivity of rocks permits its use for the temperature estimation using some empirical formula. Similar methods can be used accordingly on a regional or even global scale based on empirically matched data [28] or data determined from the global magnetovariational sounding [14]. At the same time, the complex, non-homogeneous structure of the Earth and the lack of information about its properties allow construction of only very crude temperature models based on assumptions regarding the electrical conductance mechanisms.

On the other hand, the electromagnetic (EM) sounding of geothermal areas (see, for instance, the review paper by [34], and references therein) may provide indirect temperature estimation in the Earth's interior based on electromagnetic measurements at the surface. Spichak and Zakharova [35] have developed an indirect EM geothermometer, which does not require prior knowledge or guessing regarding the electrical conductance mechanisms in the Earth's crust. In this paper, we review the application of EM geothermometry to the location of the deep heat sources, estimating dominating heat transfer mechanism at large depth and constraining location of supercritical reservoir.

## 2 Electromagnetic Geothermometry

Parameter estimation in the space between the drilled boreholes is usually carried out by linear interpolation or geostatistical tools based on the spatial statistical analysis of the approximated function, "kriging" being the most often used procedure. Using the electrical resistivity profiles revealed from the electromagnetic sounding data one could reduce the interpolation errors since in this case the database is increased due to adding new (resistivity) data related somehow to the temperature. Unlike other indirect geothermometers it enables the temperature estimation in the given locations in the earth, which makes it an indispensable tool in geothermal exploration and exploitation of the geothermal systems.

Spichak et al. [40] have shown that the temperature interpolation accuracy in the interwell space is controlled mainly by 4 factors related to the characteristics of the space between the place where the temperature profile is estimated and related EM site: faulting, meteoric and groundwater flows, spacing, and lateral geological heterogeneity (though, the latter factor being less restrictive, if appropriate EM inversion tools are used). Therefore, prior knowledge of the geology and hydrological conditions in the region under study can help to correctly locate the EM sensors with respect to the areas where the temperature is to be predicted and thereby reduce the estimation errors.

Optimal methodologies for calibration of the indirect electromagnetic geothermometer in different geological environments were developed [37, 40]. It was shown that the temperature estimation by means of the EM geothermometer calibrated by 6–8 temperature logs results in 12% average relative error. Prior knowledge of the geology and hydrological conditions in the region under study can help

to correctly locate the EM sensors with respect to the sites where the temperature is to be predicted and thereby reduce the estimation errors up to 5–6%.

Special attention was paid to the application of indirect EM geothermometer to the temperature extrapolation in depth [36]. The results obtained in the Tien Shan area indicate that the temperature extrapolation accuracy essentially depends on the ratio between the well length and the extrapolation depth. For example, when extrapolating to a depth twice as large as the well depth the relative error could be less than 2%. This result makes it possible to increase significantly the deepness of indirect temperature estimation in the earth's interior based on the available temperature logs, which, in turn opens up the opportunity to use available temperature logs for estimating the temperatures at depths, say, 3–10 km without extra drilling [29, 30].

EM geothermometry was successfully used for deep temperature assessment in the geothermal areas Soultz-sous-Forêts, France [32], Hengill, Iceland [39] and Travale, Italy [31]. Below we briefly discuss the main findings of these studies summarized in the monograph [38].

### 3 Constraining Supercritical Reservoir

It is often necessary to recognize the type of the heat carrier circulating in the geothermal system. In particular, it is difficult to distinguish between hot aqueous and gaseous fluids solely basing on the electrical resistivity and/or seismic velocities' cross-sections without prior information, which may come from geology, geochemistry, well logs, etc. However, even joint analysis of the resistivity and seismic velocities data does not always provide enough information, which might enable to draw conclusions on the type of geothermal fluids (see, for instance, [20]). On the other hand, using temperature model of the study area may provide necessary information for constraining location of geothermal reservoirs, particularly, at large depth.

This could be illustrated by the case study of the Travale geothermal area, Southern Tuscany, Italy (Fig. 1). For better understanding of the thermal structure of this area Gola et al. [17] systematized available structural, geological, geochemical, geochronological, petrological and geophysical data published by many researchers during last 30 years. According to this paper there are two main geothermal reservoirs in this area: the "shallow reservoir" hosted in the evaporite-carbonate units (about 0.7–1.0 km b.g.l. on average and with temperature from 150 °C to 260 °C) and the "deep reservoir" hosted in the metamorphic succession and Neogene granitoids (about 2.5–4.0 km b.g.l. and with temperature from 300 °C to 350 °C) [5, 27]. Fluids dominantly of meteoric origin at vapor phase circulate in both reservoirs [9]. The meteoric recharge occurs through the carbonate outcropping formations; besides a lateral input from the regional aquifers surrounding the hydrothermal reservoirs is also assumed, presumably induced by the actual exploitation process [9, 27].

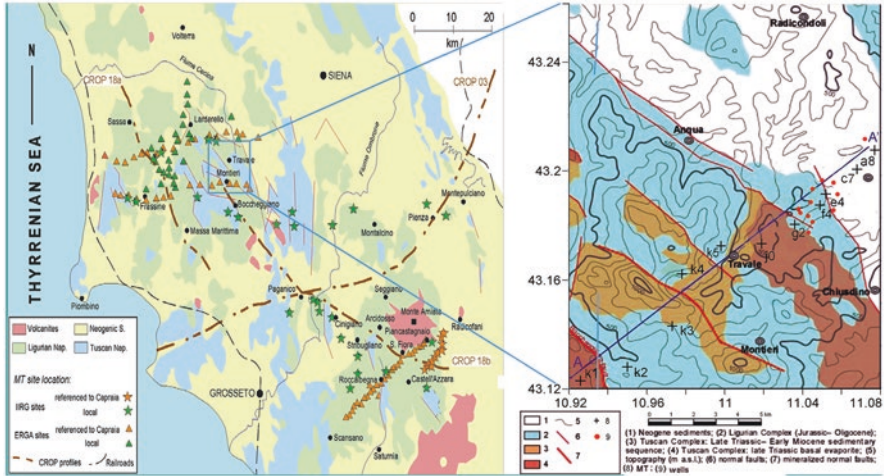


**Fig. 1** (a) The simplified tectonic scheme of the region and its location; (b) location of MT profile AA' (MT sites are marked by crosses) [7, 24]

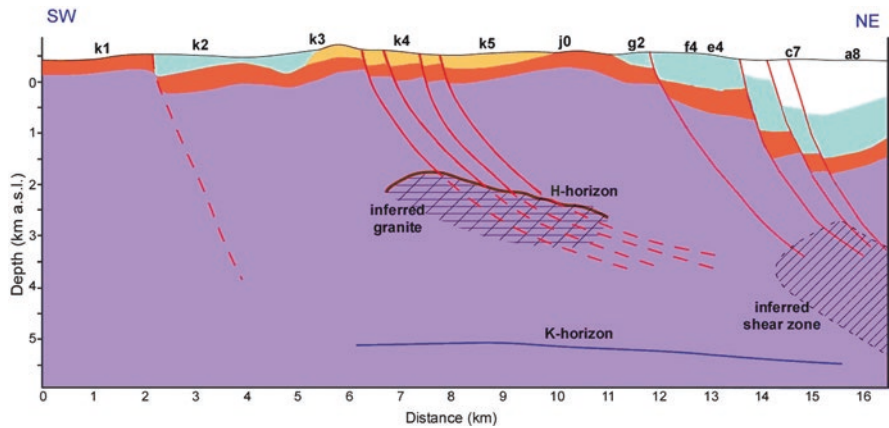


**Fig. 2** The schematic section cutting the geological structures along the eastern boundary of the Pomarance basin along AA' profile (see its location in the Fig. 1b), which accommodates the Travale geothermal anomaly (Modified after Bellani et al. [4]). The temperature isolines are marked in °C

2D and 3D seismic exploration activities carried out in the last decades provided evidences of two distinct seismic markers, referred to as “H-horizon” and “K-horizon” (shown in Fig. 2), discontinuously characterizing the entire area. Drilling data show that in some cases the H-horizon is located in correspondence of the thermo-metamorphic aureole of Neogene granitoids [6] and many wells produced super-heated steam from this level. The deeper K-horizon has similar amplitude pattern, but locally showing bright spot features and a more continuous spatial

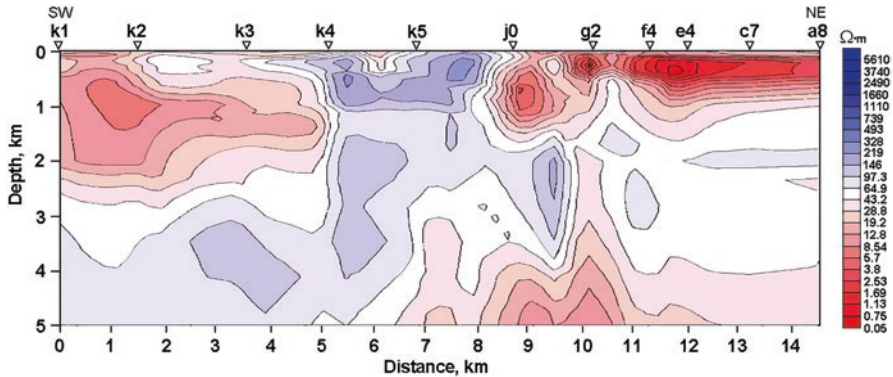


**Fig. 3** Electrical resistivity model of the Travale area along profile AA' revealed from magnetotelluric data [26]

extension with respect to H-horizon. The nature and the origin of these horizons are still under debate since 1983 (e.g., [3, 8, 23]), as it has not yet been drilled with the presumable exception of the San Pompeo 2 well. The thermobaric conditions extrapolated at this level ( $P \approx 30$  MPa and  $T > 400$  °C) do not seem to be compatible with the deep geothermal reservoir so far exploited characterized by a sub-hydrostatic pressure controlled by its current super-heated steam condition [27].

Uncertainties mentioned above could be reduced by considering the resistivity and temperature models of this area. Pushkarev [26] has built a 2D electrical resistivity model along profile AA' shown in Fig. 1b (Fig. 3). It is seen that resistivity manifests heterogeneous behavior, which correlates with large seismic anisotropy (16%) [25] and generally ranges from 10 to 100  $\Omega\cdot\text{m}$ , which indicates presence of fluid saturated rocks.

Spichak [31] has used EM geothermometer for constructing the temperature model along the same profile (Fig. 4) basing on the resistivity model mentioned above and temperature well logs available in this area. Its analysis explains the observations not addressed by previous conceptual models of this area. In particular, the isotherm  $T_{\text{SCF}} = 375$  °C characterizing possible appearance of supercritical fluids practically coincides with the upper reflection horizon H (see Fig. 2 for its location) while the isotherm  $T_{\text{BDT}} \approx 550\text{--}600$  °C characterizing granite solidus corresponds to location of the lower reflection horizon K.

These inferences could be interpreted as follows. The lower reflection horizon K marks transition from cooling partially melted magmatic intrusion (below the depth of 5 km) being in a plastic state to brittle granitic massif (above the isotherm  $T_{\text{BDT}} \approx 600$  °C) filled by mixture of deep magma waters migrated towards shallow levels, products of water – rock interaction and meteoric waters [7] being in a supercritical state under the pressure above 220 Kbar and temperature ranging between  $T_{\text{SCF}}$  and  $T_{\text{BDT}}$ . The wave velocity contrast at the lower reflection horizon K could be caused by sharp decrease of the dissimilar shear rigidity during transition from brittle to ductile medium [11].

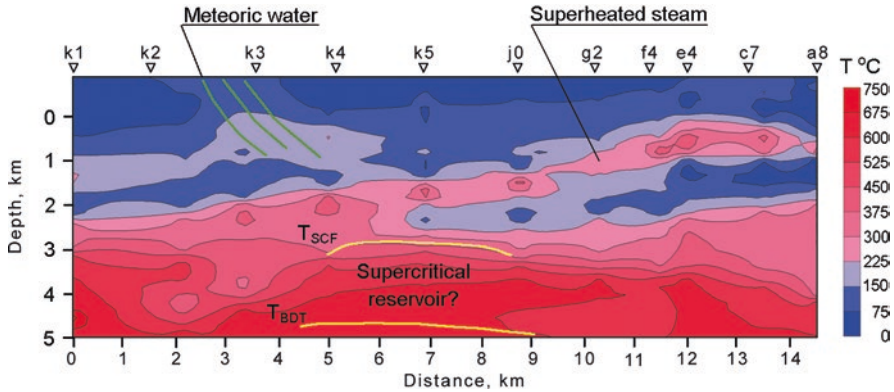


**Fig. 4** Temperature model of the Travale area along profile AA' built using EM geothermometer [31].  $T_{SCF}$  and  $T_{BDT}$  indicate locations of isotherms corresponding to supercritical fluid threshold and brittle/ductile transition, accordingly

At shallow depths ( $< 2$  km) decreasing pressure and temperatures support transition from supercritical fluids below location of the isotherm  $T_{SCF}$  and superheated mixture of steam and gas. However, this transition is not so sharp as that between brittle and ductile rocks at the depth of the isotherm  $T_{BDT}$ . Accordingly, the upper reflection horizon  $H$  separating supercritical fluids at temperatures above  $T_{SCF}$  and heavily fractured gas-steam bearing rocks manifests non-continuous behavior. It is worth mentioning in this relation that shallow (0–2 km) inclined slab beneath the sites k5-f4 (Fig. 4) often interpreted as a “shallow reservoir” (see, for instance, [17], and references therein) could be considered as a channel of transportation of the hot steam from supercritical reservoir to the surface.

## 4 Heat Sources and Seismicity

The application of the indirect EM geothermometer enables building 3-D temperature model of the study area, which could offer a comprehensive database for further analysis in geothermal terms. It was used by Spichak et al. [39] for detecting heat sources and explaining the seismicity structure in the Hengill geothermal area (Iceland).

The high-temperature Hengill area is a triple junction zone of intersection of the Western Volcanic Zone (WVZ), the Reykjanes Peninsula Rift (RPR), and the South Icelandic Seismic Zone (SISZ), which is located in the southwest of the island (Fig. 5, upper panel). The Hengill volcanic complex comprises several interconnected geothermal fields located in different directions with respect to the Mt. Hengill (marked by H in Fig. 5, lower panel): the Hveragerdi (Hv) area in the southeast; the Nesjavellir (Ne) area in the northeast, and Hellisheidi (He) area in the southwest.

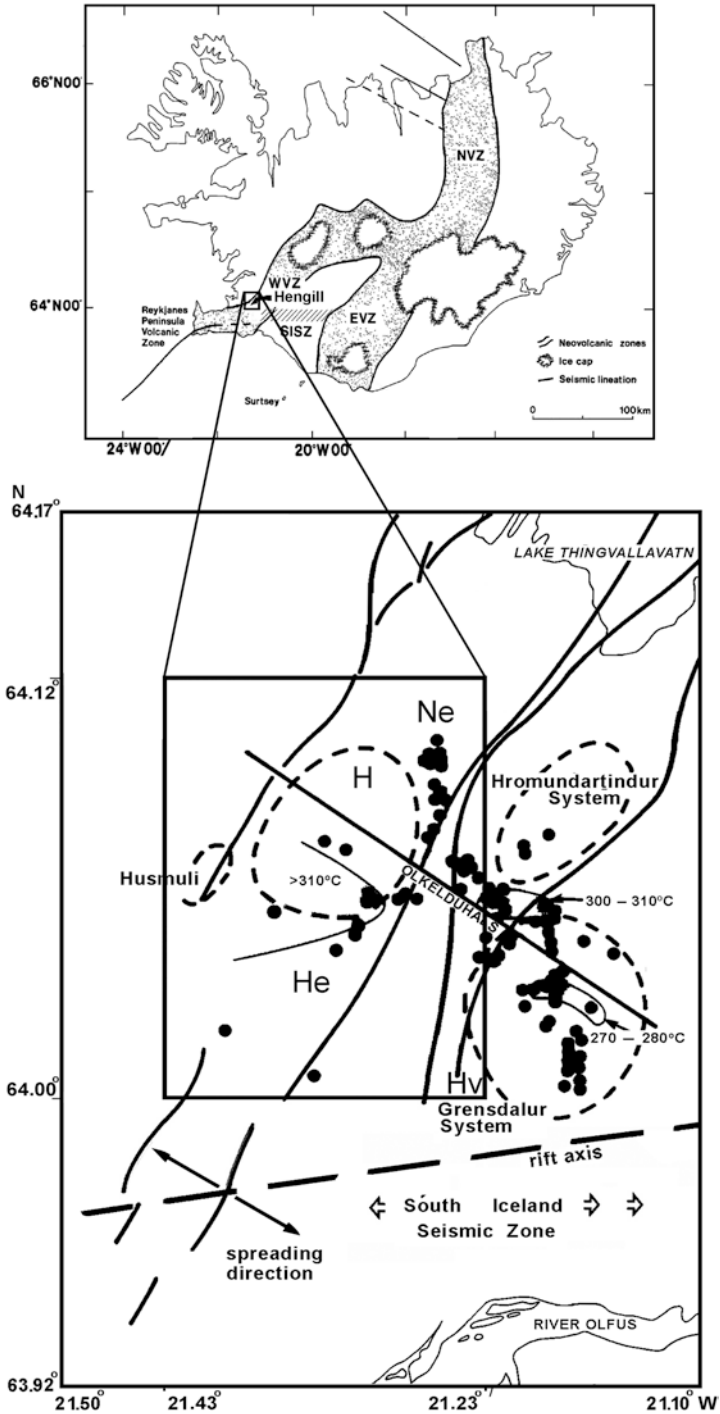


**Fig. 5** Upper panel: map of the study area. Lower panel: schematic tectonic map of the Hengill triple junction. Bold lines indicate the NNE trending eruption/fissure zones. The eruptive centers are outlined by dashed lines. Hot springs and fumaroles are indicated by dots. The line connecting the Hengill and Grendalur volcanoes indicates the axis of the transverse tectonic structure. Rectangle bounds the studied area. (Modified from Foulger and Toomey [16])

Overall, the region and its immediate vicinity hosts four centers of volcanic activity (Fig. 5, lower panel): the Hengill area mentioned above, as well as the Grensdalur, Hromundartindur, and Husmuli areas. The Hengill volcanic complex comprises an active central volcano and a swarm of fractures trending north-northeastwards (Fig. 6). The secondary tectonic structural trend, transverse to the dominant NNE-SSW trend of the signs of crustal accretion, has developed in the zone connecting the centers of the Hengill and Grensdalur volcanic complexes and extending along the Olkelduhals line (Fig. 5, lower panel).

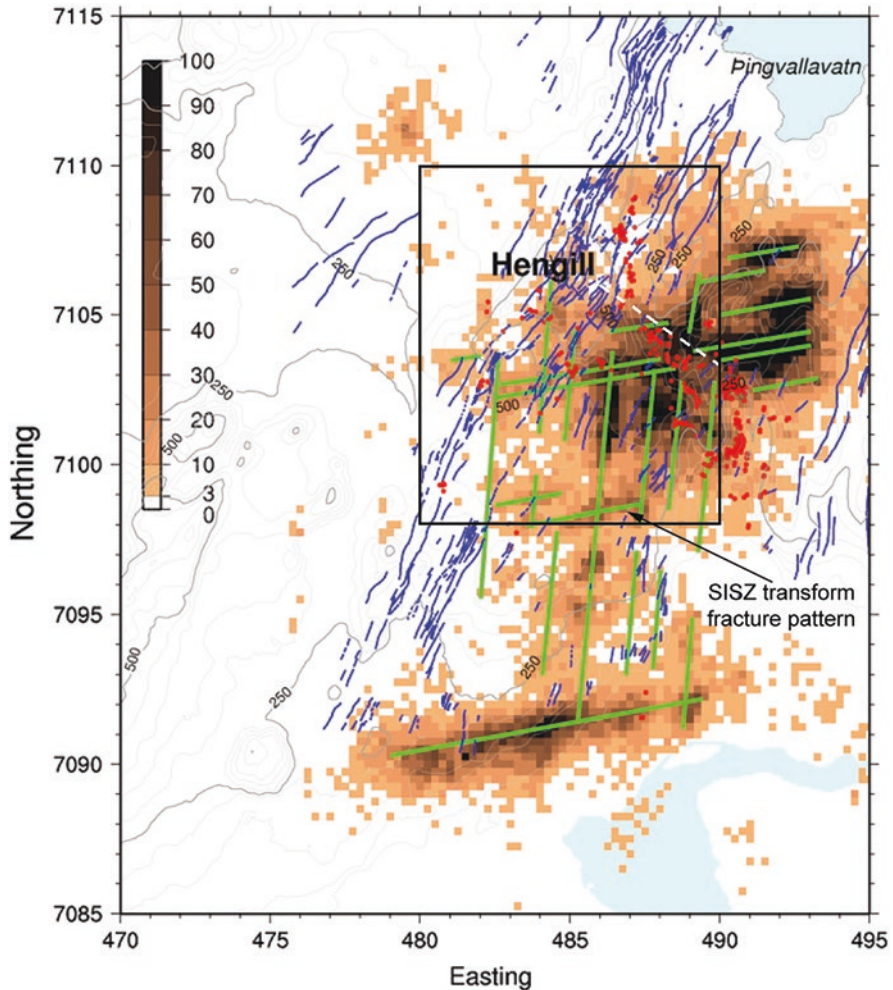


**Fig. 6** Density of seismic epicenters from 1991 to 2001 and inferred transform tectonic lineaments (thick lines) based on the overall distribution of the seismicity (thin lines - faults and fissures mapped on the surface). Rectangle bounds the studied area indicated in the Fig. 5. (Redrawn from Árnason et al. [1])



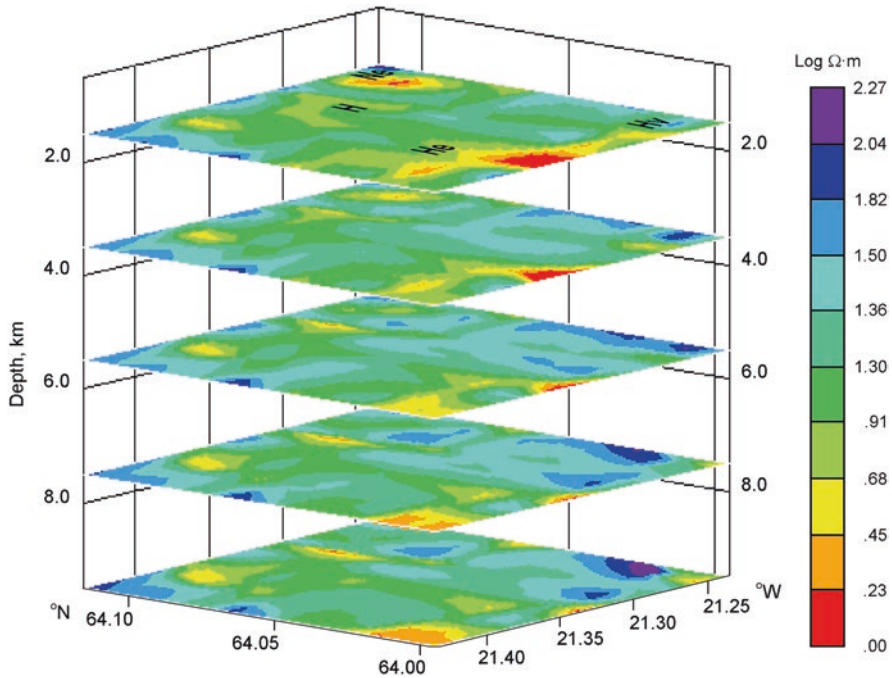
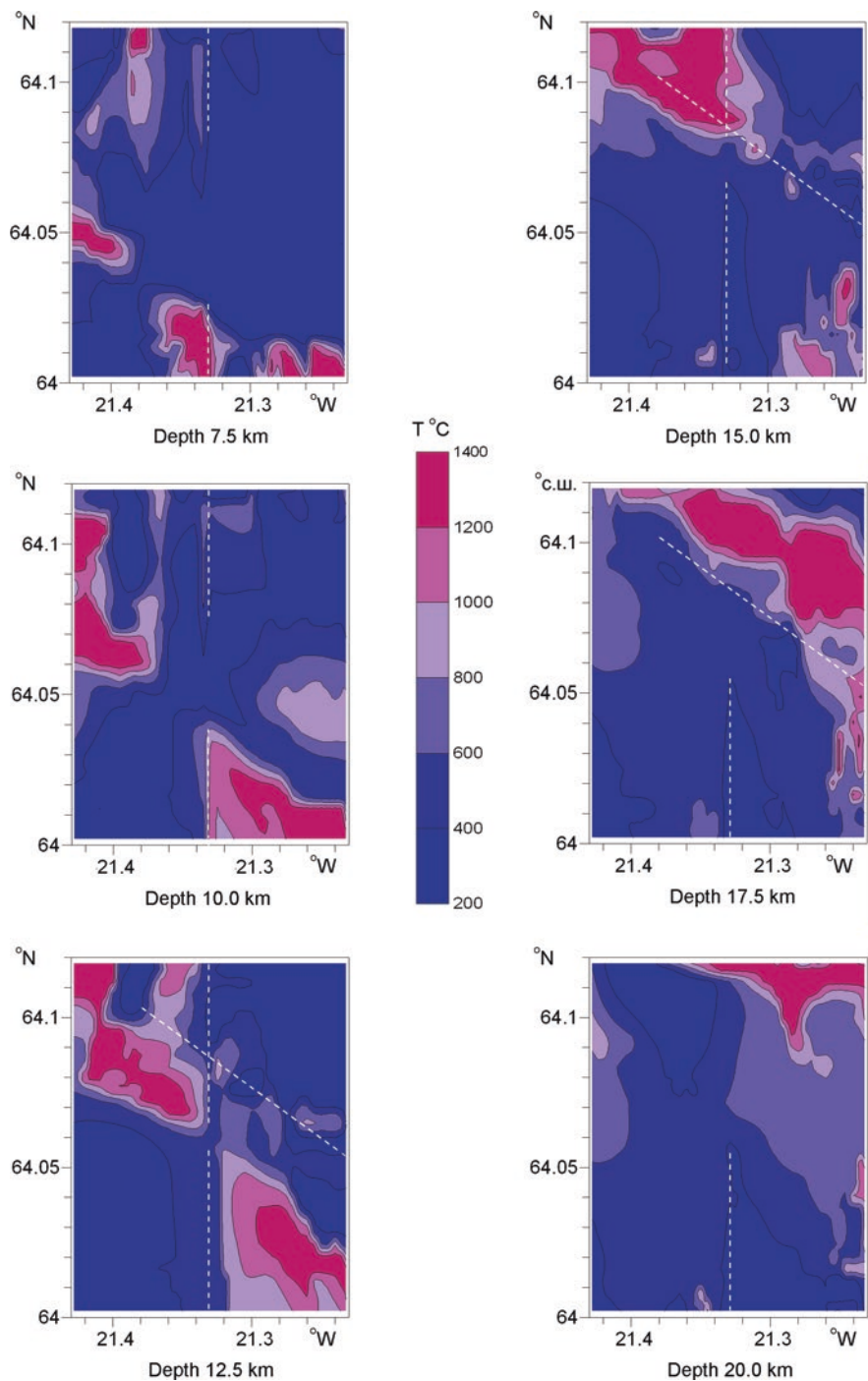


Fig. 7 Slices of the electrical resistivity distribution in the Hengill area at different depths [33]

Spichak et al. [33] have built 3-D electrical resistivity model of the Hengill geothermal area up to the depth of 20 km (Fig. 7). Basing on this model the authors indicated that the heat source in the upper crust of the region could be the upflow of highly conductive material from below 20 km, its accumulation in the subsurface reservoirs and further spreading in the rheologically weak layer at depths 5–15 km. The obtained results confirm the mantle origin of the heat sources in this region, which was hypothesized earlier. Meanwhile, no continuous well conductive layer with resistivities less than 10 Ohm.m is detected in the depth range 10–25 km. Instead local well conducting areas were found linked with each other both in horizontal and vertical directions.

Spichak et al. [39] have constructed the first 3-D temperature model of the Hengill geothermal area (Figs. 8 and 9). The analysis of the temperature model enabled to draw important conclusions about the structure of this geothermal area, location of heat sources, seismicity pattern, etc., and formulate a new conceptual model of the Icelandic crust. According to this model the background temperature of the Icelandic crust above 20 km does not exceed 400°C. It is overlapped by a network of interconnected high-temperature low resistive channels, which braid through the crust mainly at a level of 10–15 km and root to a depth greater than 20 km.

Accordingly, the probable heat sources feeding the geothermal system are supposed to be the intrusions of the hot partially molten magma upwelling from the mantle through the faults and fractures. In particular, it was inferred that the



**Fig. 8** Slices of the temperature distribution in the Hengill area at different depths [39]. Vertical dashed line indicates the hypothesized location of the deep transform fault; diagonal dashed line marks the projection of the Olkelduhals transverse tectonic structure indicated in the Figs. 5–6

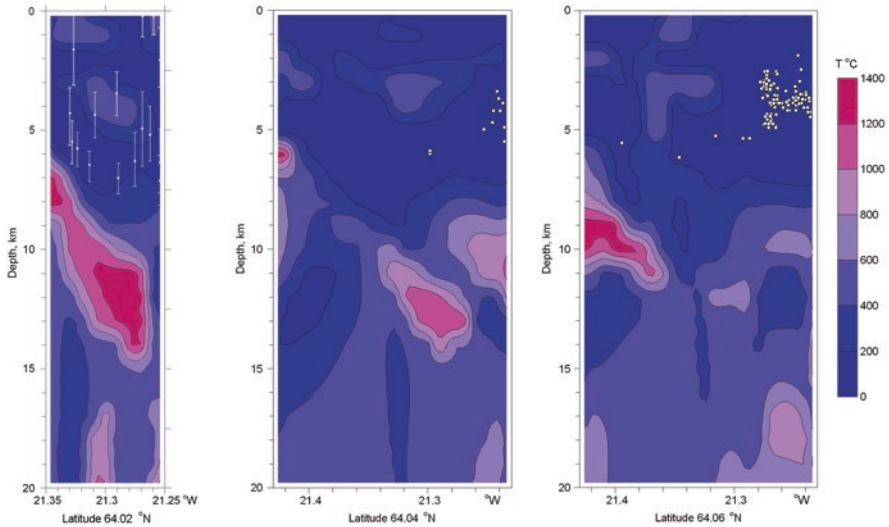


**Fig. 9** Temperature cross-sections in the Hengill area at different latitudes. Bars are redrawn from Stefansson et al. [41]. White dots indicate the earthquake hypocenters according to Jousset et al. [20]

unusually high temperatures (1100 °C) detected at the depth 2 km of the study area [15] could originate from the molten liquid magma (with temperature higher than liquidus) upwelling from the mantle and finally accumulating in the shallow magma pockets at depths 2–5 km (Fig. 9). The comparison between the vertical temperature cross-sections and the projections of the earthquake hypocenters showed that they all are located in the areas where temperature does not exceed 400°C (see locations of hypocenters in the Fig. 9), which is a gabbro solidus in a silica-rich Icelandic crust.

Joint analysis of the temperature and resistivity models together with the gravity data enabled to discriminate the locations of relict and active parts of the volcanic geothermal complex. Figure 10 indicates Bouguer gravity anomaly map, where four adjacent domains (see their locations in Fig. 5, lower panel) correspond to the regions in the crust with different thermal regimes: in the Husmuli (I) and Grensdalur (III) large massifs of the solidified magma are cooling while in more active Nesjavellir (II) and Hellisheidi (IV) areas the upwelling of the partially molten magma or hot fluids takes place. They are separated by a deep SN fault and the Olkelduhals transverse tectonic structure (marked in the Fig. 10 by dashed lines). The deep fault is traced in the horizontal slices of both electrical resistivity (Fig. 7) and temperature (Fig. 8) and coincides with the supposed location of the hypothesized transform fault submeridionally striking in the southern part of the region (Fig. 6).

This, in turn, explains the observed seismicity pattern by different geothermal regimes in four adjacent parts of the area separated by the deep S–N fault constrained between the meridians 21.31° and 21.33°W and a WNW–ESE diagonal band running beneath the second-order tectonic structure of Olkelduhals.

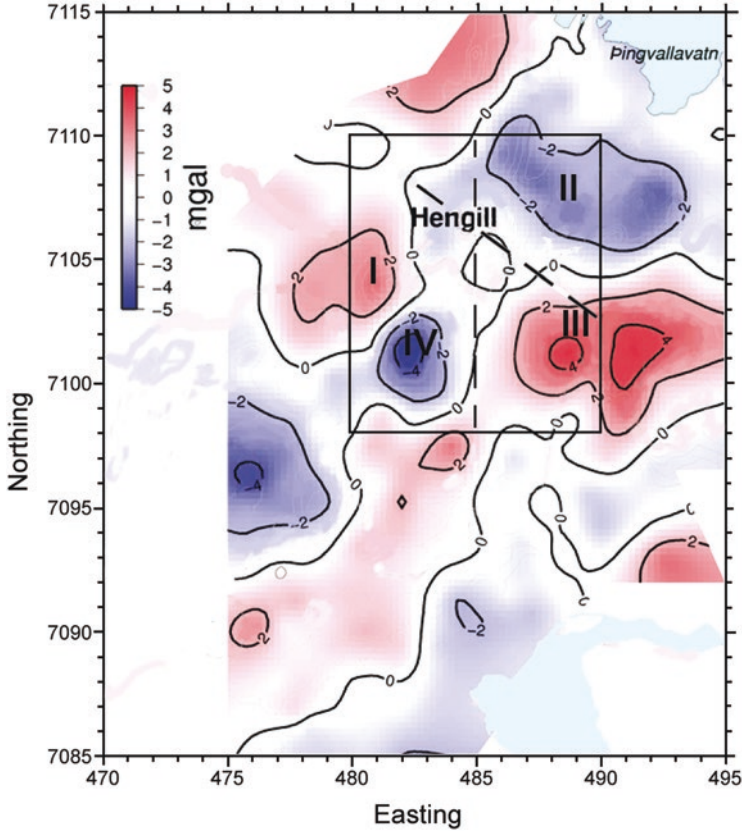


**Fig. 10** Residual Bouguer anomaly map (Modified after Árnason et al. [1]); I-IV indicate gravity anomalies; vertical dashed line indicates projection of the deep resistivity and temperature fault; diagonal dashed line marks the axis of the Olkelduhals transverse tectonic structure. Rectangle bounds the studied area

## 5 Estimating the Dominating Heat Transfer Mechanism and Fluid Circulation Paths

An indirect electromagnetic geothermometer was used by Spichak et al. [32] for deep temperature estimations in the Soultz-sous-Forêts geothermal area (France) (Fig. 11) using magnetotelluric (MT) sounding data collected along the profile AB. Validation of temperature assessment carried out by comparison of the forecasted temperature profile with temperature log from the deepest borehole has resulted in the relative extrapolation accuracy less than 2%. It was found that the resistivity's uncertainty caused by MT inversion errors and by possible effects of external factors very weakly affects the resulting temperature, the latter being influenced mainly by the ratio between the borehole and extrapolation depths.

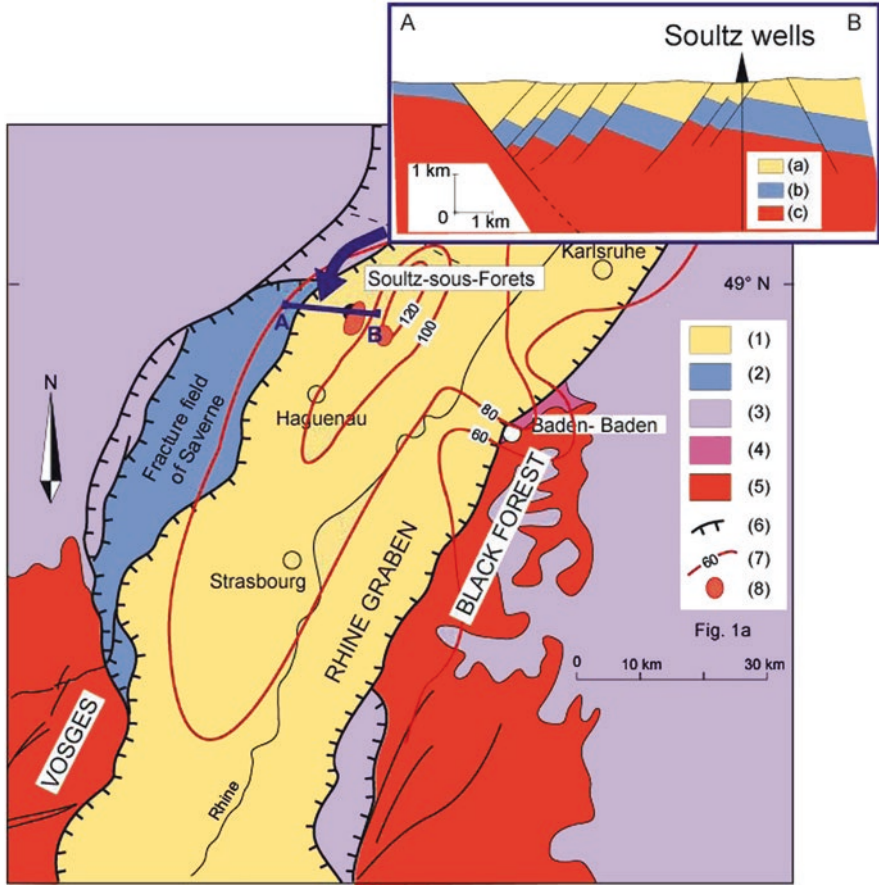


**Fig. 11** Location of the EGS Sultz site and geology of the Upper Rhine Graben: (1) Cenozoic sediments, (2) Jurassic, (3) Trias, (4) Permian, (5) Hercynian basement, (6) Border faults, (7) Temperature distribution in °C at 1500 m depth [18], (8) Local thermal anomalies [18]. Simplified cross-section through profile AA': (a) Cenozoic filling sediments (b) Mesozoic sediments, (c) Paleozoic granite basement [12]

2D inversion of MT data has resulted in the electrical resistivity section along profile AB (Fig. 12). Application of EM geothermometer enabled to build the temperature cross-section up to the depth 5000 m (Fig. 13). It manifests local temperature maxima at large depths beneath the wells GPK2 and RT1/RT3 indicating appropriate heat sources located at large depths.

Another remarkable feature of the temperature cross-section concerns to the isotherms' sinusoidal shape in the horizontal direction that supports the hypothesis on the deep rooted fluid circulation in the Sultz fractured granitic basement [10, 22]. The analysis of the temperature profile in GPK2 location beneath 5000 m has shown

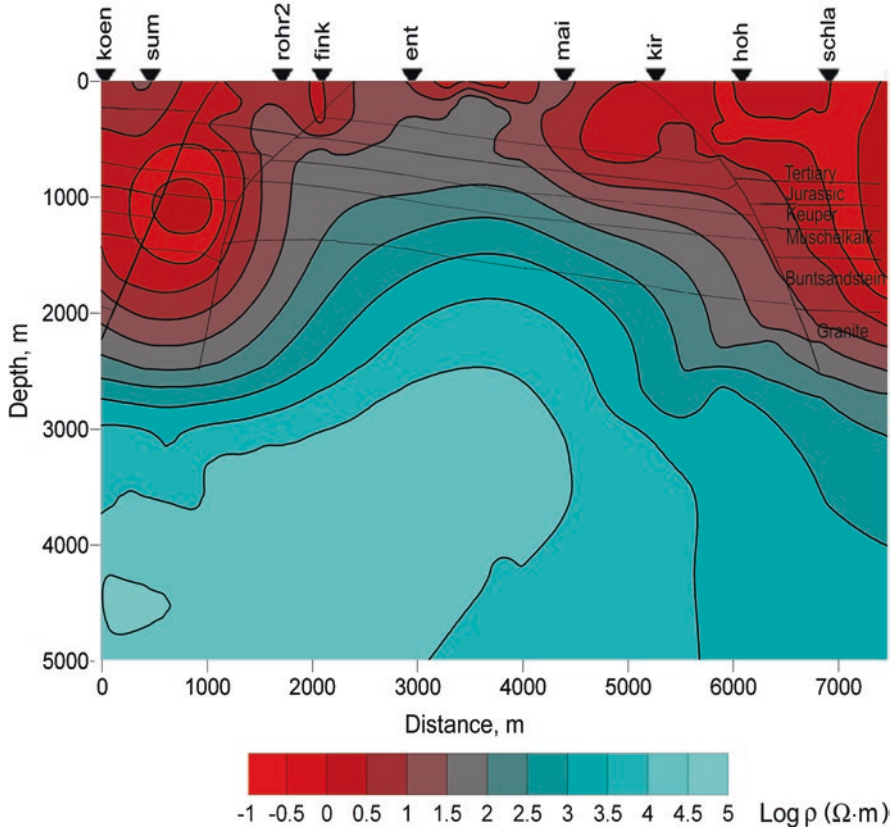


**Fig. 12** Electrical resistivity cross-sections along the profile AA' (Sultz-sous-Forêts, France) [32]. Triangles indicate locations of MT sites

that its behavior continues to be of the conductive type (as in the depth range 3700–5000 m) up to the depth 6000 m, while manifesting convective type below this depth (Fig. 14b).

It is worth mentioning in this connection that a common way of searching for the fluid circulation paths at large depths basing only on the electrical resistivity cross-sections (see, for instance, [24]) may lead to incorrect inferences, since the low resistivity anomalies could be caused by a number of reasons. Using of the temperature cross-sections may reduce the uncertainty and help to trace the fluid flows (see previous sections).

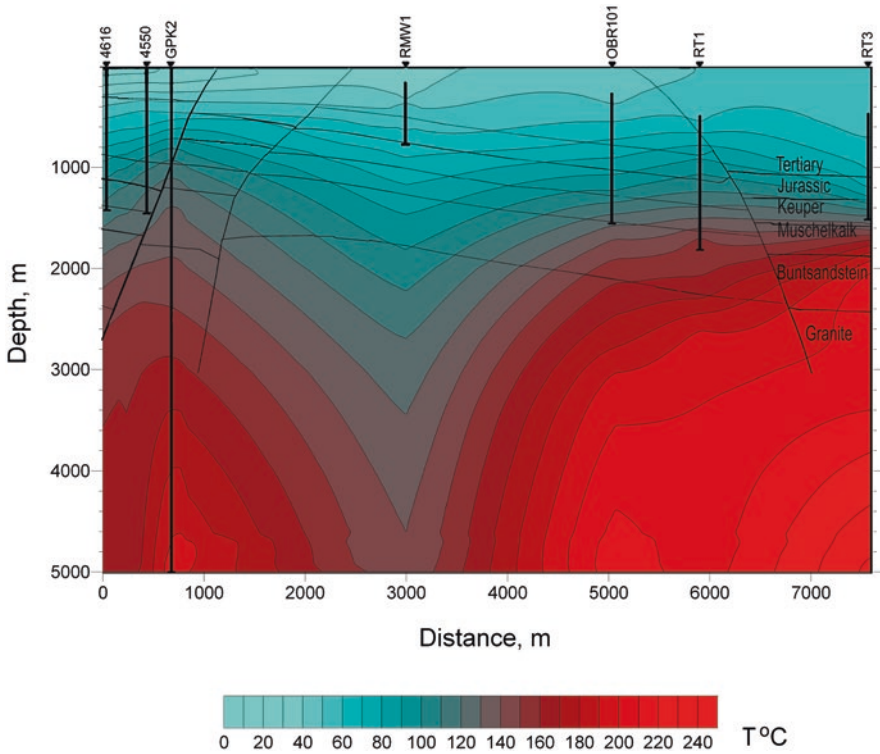


**Fig. 13** Temperature cross-section along the profile AA' (Soultz-sous-Forêts, France) [32]. Vertical solid lines indicate boreholes' locations in the vicinity of the profile AA'

## 6 Conclusions

The studies carried out using indirect EM geothermometer lead to the following conclusions.

The temperature estimates obtained with indirect EM geothermometers could be based on its advance calibration of electrical resistivity - temperature relationships in a few wells. Due to this the temperature estimates do not depend explicitly on alteration mineralogy or other factors influencing the temperature reconstruction in different geological environments.

The temperature interpolation accuracy in the interwell space is controlled mainly by 4 factors related to the characteristics of the space between the place where the temperature profile is estimated and related EM site: faulting, meteoric and groundwater flows, spacing, and lateral geological heterogeneity (though, the latter factor being less restrictive, if appropriate EM inversion tools are used). Therefore, prior knowledge of the geology and hydrological conditions in the region under study can help to correctly locate the EM sensors with respect to the areas where the temperature is to be predicted and thereby reduce the estimation errors.

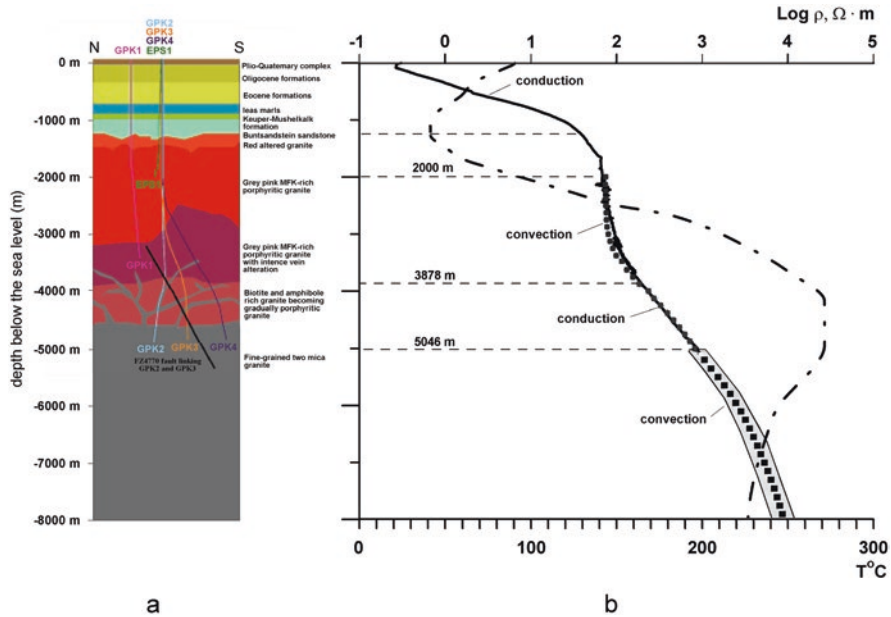


**Fig. 14** (a) 2D conceptual model of the geology at Soultz-sous-Forets (modified after [13]); (b) temperature extrapolation in the well GPK2 for the depth range 5046 m – 8175 m. The temperature well log is indicated by solid line, forecasted temperature – by crosses, log resistivity profile is marked by dashed – dotted line. Hatched area indicates the bars corresponding to 10% uncertainty in the resistivity model used for the temperature forecast. (Modified after Spichak et al. [32])

Application of the indirect electromagnetic geothermometer allows high accuracy temperature estimation at depths exceeding the depths of drilled wells for which temperature data are available. Electromagnetic geothermometer could provide the spatial temperature models in the absence of manifestations of geothermal activity on the surface. They, in turn, offer a comprehensive database for drawing conclusions regarding location of the heat sources, fluid type and its circulation paths, and supercritical fluids at large depths not accessible by available boreholes.

**Acknowledgements** This study was carried out partly due to support of RSCF (grant N20-17-00155).

**References**

1. Árnason KH, Eysteinnsson E, Hersir GP (2010) Joint 1D inversion of TEM and MT data and 3D inversion of MT data in the Hengill area, SW Iceland. *Geothermics* 39:13–34
2. Arnorsson S, Gunnlaugsson E (1985) New gas geothermometers for geothermal exploration-calibration and application. *Geochim Cosmochim Acta* 49(6):1307–1325



3. Batini F, Bertini G, Bottai A et al (1983) San Pompeo 2 deep well: a high temperature and high pressure geothermal system. In: Extended abstract of third international seminar on results of EC research and demonstration projects in the field of geothermal energy: 341–353
4. Bellani S, Brogi A, Lazzarotto A et al (2004) Heat flow, deep temperatures and extensional structures in the Larderello geothermal field (Italy): constraints on geothermal fluid flow. *J Volcanol Geotherm Res* 132:15–29
5. Bertani R, Bertini G, Cappetti G et al (2005) An update of Larderello-Travale/Radicondoli deep geothermal system. In: Extended abstract for the world geothermal congress, Antalya, Turkey
6. Bertini G, Casini GG et al (2006) Geological structure of a long-living geothermal system, Larderello, Italy. *Terra Nova* 18(3):163–169
7. Brogi A, Lazzarotto A, Liotta D et al (2005) Crustal structures in the geothermal areas of southern Tuscany (Italy): insights from the CROP 18 deep seismic reflection lines. *J Volcanol Geotherm Res* 148:60–80
8. Cameli GM, Dini I, Liotta D (1993) Upper crustal structure of the Larderello geothermal field as a feature of post-collisional extensional tectonics, Southern Tuscany, Italy. *Tectonophysics* 224(4):13–423
9. Celati R, Cappetti G, Calore C et al (1991) Water recharge in Larderello geothermal field. *Geothermics* 20:119–133
10. Clauser C, Villinger H (1990) Analysis of conductive and convective heat transfer in a sedimentary basin, demonstrated for the Rhein graben. *Geophys J Intern* 100:393–414
11. Carzione JM, Poletto F (2013) Seismic rheological model and reflection coefficients of the brittle-ductile transition. *Pure Appl Geophys* 170:2021–2035
12. Dezayes C, Chevremont P, Tourliere B et al (2005) Geological study of the GPK4 HFR borehole and correlation with the GPK3, borehole (Soulz-sous-Forets, France). BRGM/RP-53697-FR. Technical Report, BRGM
13. Dezayes C, Genter A, Hooijkaas G (2005) Deep-seated geology and fracture system of the EGS Soutz reservoir (France) based on recent 5km depth boreholes. In: Proceedings of the world geothermal congress, Antalya, Turkey
14. Dmitriev VI, Rotanova NM, Zakharova OK (1988) Estimations of temperature distribution in transient layer and lower mantle of the Earth from data of global magnetovariational sounding. *Izvestiya RAN ser Fizika Zemli* 2:3–8. (in Russian)
15. Elders WA, Fridleifsson GO (2010) The science program of the Iceland Deep Drilling Project (IDDP): a study of supercritical geothermal resources. In: Expanded abstracts of the world geothermal congress, Bali, Indonesia
16. Foulger GR, Toomey DR (1989) Structure and evolution of the Hengill-Grensdalur volcanic complex, Iceland: geology, geophysics, and seismic tomography. *J Geophys Res* 94(B12):17511–17522
17. Gola G, Bertini G, Bonini M et al (2017) Data integration and conceptual modeling of the Larderello geothermal area, Italy. *Energy Procedia*. <https://doi.org/10.1016/j.egypro.2017.08.201>
18. Haenel R, Legrand R, Balling N et al (1979) Atlas of subsurface temperatures in the European Community. Th. Schafer Druckerei GmbH, Hannover
19. Harvey CC, Browne PRL (1991) Mixed-layer clay geothermometry in the Wairakei geothermal field, New Zealand. *Clays Clay Miner* 39:614–621
20. Jousset P, Haberland C, Bauer K et al (2011) Hengill geothermal volcanic complex (Iceland) characterized by integrated geophysical observations. *Geothermics* 40:1–24
21. Kharaka YK, Mariner RH (1989) Chemical geothermometers and their application to formation waters from sedimentary basins. In: Naeser ND, McCulloch T (eds) *Thermal history of sedimentary basins*. S.C.P.M. Special issue, Springer, pp 99–117
22. Le Carlier C, Royer JJ, Flores EL (1994) Convective heat transfer at Soultz-sous-Forêts geothermal site: implications for oil potential. *First Break* 12(11):553–560
23. Liotta D, Ranalli G (1999) Correlation between seismic reflectivity and rheology in extended lithosphere: southern Tuscany, inner Northern Apennines, Italy. *Tectonophysics* 315:109–122

24. Manzella A, Spichak V, Pushkarev P et al (2006) Deep fluid circulation in the Travale geothermal area and its relation with tectonic structure investigated by a magnetotelluric survey. In: Expanded abstracts of the 31th workshop on geothermal reservoir engineering, Stanford University, USA
25. Piccinini D, Saccorotti G (2018) Observation and analysis of shear wave splitting at the Larderello-Travale geothermal field, Italy. *J Volcanol Geotherm Res* 363:1–9
26. Pushkarev PY (2007) 2D resistivity model of the Travale geothermal field revealed from MT data. In: Proceeding of the workshop INTAS project, Pisa, Italy
27. Romagnoli P, Arias A, Barelli A et al (2010) An updated numerical model of the Larderello-Travale geothermal system, Italy. *Geothermics* 39:292–313
28. Shankland T, Ander M (1983) Electrical conductivity, temperatures, and fluids in the lower crust. *J Geophys Res* 88(B11):9475–9484
29. Spichak VV (2013) A new strategy for geothermal exploration drilling based on using of an electromagnetic sounding data. In: Expanded abstract of the international workshop on high enthalpy geothermal systems. San-Bernardino, California
30. Spichak VV (2014) Reduce geothermal exploration drilling costs: pourquoi pas?! In: Expanded abstract of the D-GEO-D conference, Paris, France
31. Spichak VV (2019) Temperature models of geothermal areas: lessons learned from electromagnetic geothermometry. In: Proc. Int. Workshop on Water Dynamics. Sendai, Japan
32. Spichak V, Geiermann J, Zakharova O et al (2015) Estimating deep temperatures in the Soultz-sous-Forêts geothermal area (France) from magnetotelluric data. *Near Surface Geophys* 13(4):397–408
33. Spichak V, Goidina A, Zakharova O (2011) 3D geoelectrical model of the Hengill volcanic complex (Iceland). *Trans KRAUNZ* 1(19):168–180. (in Russian with English abstract)
34. Spichak VV, Manzella A (2009) Electromagnetic sounding of geothermal zones. *J Appl Geophys* 68:459–478
35. Spichak VV, Zakharova OK (2007) Temperature estimation in the earth's interior from the ground electromagnetic sounding data. *Izvestiya Phys Solid Earth* 6:68–73
36. Spichak VV, Zakharova OK (2009) The application of an indirect electromagnetic geothermometer to temperature extrapolation in depth. *Geophys Prospect* 57:653–664
37. Spichak VV, Zakharova OK (2012) The subsurface temperature assessment by means of an indirect electromagnetic geothermometer. *Geophysics* 77(4):WB179–WB190
38. Spichak VV, Zakharova OK (2015) Electromagnetic geothermometry. Elsevier, Amsterdam
39. Spichak VV, Zakharova OK, Goidina AG (2013) A new conceptual model of the Icelandic crust in the Hengill geothermal area based on the indirect electromagnetic geothermometry. *J. Volcanol/Geotherm Res* 257:99–112
40. Spichak VV, Zakharova OK, Rybin AK (2011) Methodology of the indirect temperature estimation basing on magnetotelluric data: northern Tien Shan case study. *J Appl Geophys* 73:164–173
41. Stefansson R, Gudmundsson JB, Roberts MJ (2006) Long-term and short-term earthquake warnings based on seismic information in the SISZ. In: Veðurstofa Íslands – Greinargerð, Icelandic Meteorological Office, Rep. 06006, 53 pp. Reykjavik